Structural and Redox Properties of the $La_{(1-x)}Sr_xMn_{0.5}Co_{0.5}O_3$ (x = 0.0, 0.1, 0.2, 0.3, 0.4, 0.5) Nano-Catalysts for Carbon Monoxide Oxidation

M. Lotfi[a], A. Gholizadeh[a,*], A. Malekzadeh[b]

[a] *School of Physics, Damghan University (DU), Damghan, I. R. Iran.*
[b] *School of Chemistry, Damghan University (DU), Damghan, I. R. Iran.*

ARTICLE INFO

ABSTRACT

Structural features of the $La_{(1-x)}Sr_xMn_{0.5}Co_{0.5}O_3$ (x = 0.0, 0.1, 0.2, 0.3, 0.4, and 0.5) nano-particles were investigated using X-ray powder diffraction and FT-IR spectroscopy. The characterization of compounds by X-ray powder diffraction and using Fullprof program show a cubic structure (Pm3m space group) for x = 0.0 and a rhombohedra structure (R-3c space group) for the Sr substituted $La_{(1-x)}Sr_xMn_{0.5}Co_{0.5}O_3$ samples. Crystallite size and unit cell parameters decrease with Sr substitution. The electrical conductivity of the samples in oxidizing (air) and reducing atmosphere (6% CO in nitrogen) as well as band gap of the samples have been investigated to interpret the performance of the samples. Results show that their behavior is enhanced non-uniformly with increase in Sr substitution. An increase of Sr substitution up to 0.5 enhances the performance of the samples and an optimal catalytic activity in the low-temperature conversion of CO to CO_2. It is mainly attributed to a decrease of the crystallite size.

1. Introduction

From 1970's decade, automakers have designed a catalytic transducer to reduce air pollutants caused by exhausted gas from automobiles. A considerable amount of gaseous pollutants is removed during the passage of the transducer [1.]. Many efforts have been made to reduce the use of precious metals of Pt, Pd, and Rh in catalysts, and finding a suitable replacement to further reduce environmental pollutants emitted is a main research in the modern world. High activity in redox reaction, oxygen storage capability and high flexibility to enter other metals in structure, has proposed perovskite compounds, with the formula ABO_3, as a good candidate for this replacement. The catalytic properties of perovskites depend on the nature of the cations A and B. Lanthanum manganite ($LaMnO_3$) and lanthanum cobaltite ($LaCoO_3$) are among the famous perovskites that are used for complete oxidation of carbon monoxide [2,3].

The mixture of lanthanum with cobalt and manganese ions with the formula $LaMn_{1-y}Co_yO_3$ is known as manganite-cobaltite. In these compounds, the origin of metal-ferromagnetic behavior is due to ferromagnetic interaction between Mn^{3+}-Mn^{3+} and Mn^{4+}-Co^{2+} cations [4]. Cations of Co and Mn may exist in many different states in $La_{1-x}M_xMn_{1-y}Co_yO_3$ perovskites. Thus, there may be many possible ways for Co-Mn cations interaction to take place via oxygen and a complete understanding of the magnetic state of such system is not easy

Corresponding author:
E-mail address: gholizadeh@du.ac.ir (Ahmad Gholizadeh).

Table 1. Experimental conditions for the preparation of $La_{1-x}Sr_xMn_{0.5}Co_{0.5}O_3$ samples[a]

Sample	Mole of $La(NO_3)_3 \cdot 6H_2O$	Mole of $Sr(NO_3)_2$	Mole of $Co(NO_3)_2 \cdot 6H_2O$	Mole of $Mn(NO_3)_2 \cdot 4H_2O$
x = 0.0	0.0164	-----	0.00820	0.00820
x = 0.1	0.0150	0.00167	0.00837	0.00837
x = 0.2	0.0136	0.00324	0.00855	0.00855
x = 0.3	0.0122	0.00524	0.00876	0.00876
x = 0.4	0.0107	0.00716	0.00895	0.00895
x = 0.5	0.0092	0.00916	0.00916	0.00916

[a]mole of the citric acid is considered to be 0.081 in all preparation

[4]. In this work, structural, redox and catalytic properties of the $La_{1-x}Sr_xMn_{0.5}Co_{0.5}O_3$ (x = 0.0, 0.1, 0.2, 0.3, 0.4, 0.5) nano-perovskites have been synthesized by the citrate method, characterized and investigated for complete oxidation of carbon monoxide.

2. Experimental
The samples of $La_{1-x}Sr_xMn_{0.5}Co_{0.5}O_3$ (x = 0.0, 0.1, 0.2, 0.3, 0.4, 0.5) were prepared by the citrate method. Firstly, a solution made of proper moles number of $La(NO_3)_3 \cdot 6H_2O$, $Mn(NO_3)_2 \cdot 4H_2O$, $Co(NO_3)_2 \cdot 6H_2$, $Sr(NO_3)_2$ according to Table 1, in 20 ml distilled water and citric acid (equal to the total number of moles of nitrate ions) was evaporated at 80, 150 and 200°C overnight. The samples were completely powdered after each drying. The resulting materials were powdered and calcined at 600 and 900°C for 5 h, respectively.

The X-ray diffraction (XRD) patterns have been recorded with a Bruker AXS diffractometer D8 ADVANCE with Cu-Kα radiation in the range 2θ = 20-80°. The XRD data were analyzed using a commercial X'pert package and Fullprof program. Crystallite sizes were calculated by the XRD data using Scherer's equation. The FT-IR spectra of the samples were recorded with a PERKIN-ELMER FT-IR spectrometer in the wavenumber range of 400-4000 cm^{-1}. The particle size of the samples was investigated by TEM (LEO Model 912AB) analysis. Absorption coefficient is a suitable quantity for studying the band gap energy. Optical absorption spectra of the samples between 200

and 1000 nm wavelengths have been recorded with a HP-UV–Vis system (Agilent8453, model). Band gap energies have been calculated according to Ref. [5]. A quartz tube with two extra pure gold wires as electrode parallel to each other, inserted in either side of inner wall of the cell, was used for electrical conductivity measurements. The electrical conductivity of the samples in air atmosphere (oxidizing conditions) has been studied from lab temperature to a final temperature by a randomly increasing the temperature to 350°C. Reducibility properties of catalysts were studied by electrical conductivity measurements in oxidation (air) and reduction (6%CO in Ar) atmosphere under steady state conditions at 350°C.

The performance of catalysts for complete oxidation of CO was studied in a typical experiment of a mixture of 6%CO in Ar and air in a total gas mixture flow rate of 47 cm^3/min. The catalytic test studies were carried out by temperature rising in random intervals from 30°C to complete oxidation temperature.

3. Results and Discussion
X-ray diffraction patterns of the $La_{1-x}Sr_xMn_{0.5}Co_{0.5}O_3$ (x = 0.0, 0.1, 0.2, 0.3, 0.4, 0.5) compounds are shown in Figure 1. The XRD data were analyzed using both the commercial X'Pert High Score package and Fullprof program. Identification of the structure type using X'Pert package confirms perovskite structure in all samples without presence of impurity phases. Results of the Rietveld analysis using Fullprof program indicate that

Table 2. The values of crystallite size and unit cell parameters of $La_{1-x}Sr_xMn_{0.5}Co_{0.5}O_3$ samples

Sample	D (nm)	$(b_H=) a_H(\text{Å})$	$c_H(\text{Å})$	$V_H(\text{Å}^3)$
x = 0.1	22.0	5.472	13.246	343.484
x = 0.2	19.6	5.461	13.256	342.36
x = 0.3	17.8	5.434	13.397	342.59
x = 0.4	15.7	5.455	13.217	340.6
x = 0.5	15.7	5.447	13.229	339.916

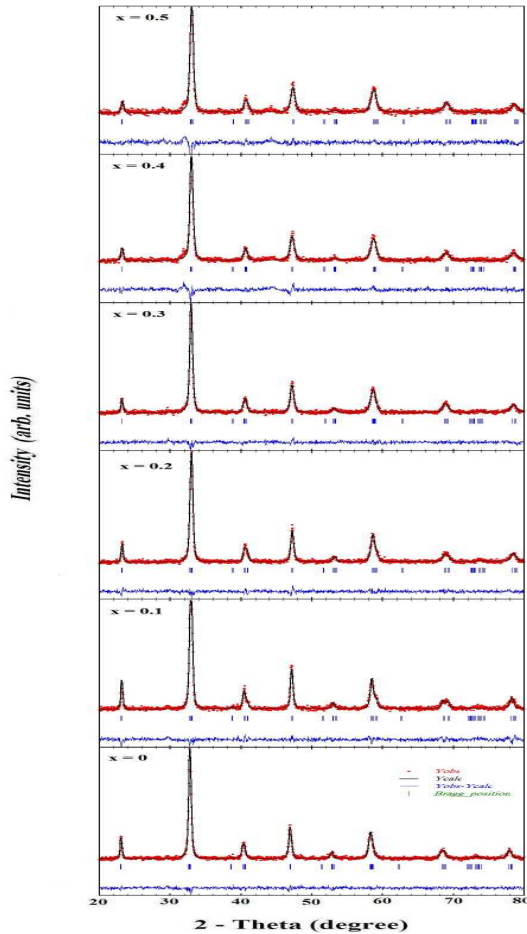**Fig. 1.** Rietveld analysis of the X-ray diffraction patterns for the $La_{1-x}Sr_xMn_{0.5}Co_{0.5}O_3$ samples. The circle sings represent the raw data. The solid line represents the calculated profile. Vertical bars indicate the position of Bragg peaks for samples with the rhombohedra structure (Space Group R-3c) and for sample x = 0.0 with the cubic structure (Space Group Pm3m). The lowest curve is the difference between the observed and the calculated patterns.

all the diffraction peaks of the sample with x = 0.0 can be quite well indexed in cubic structure (space group Pm3m), and for other samples in Rhombohedra structure (space group R-3c). The best fit with the least difference is carried out as shown in Figure 1. The values of the crystallite sizes obtained from ((104), 2θ = 32.8°) peak using Scherer method and lattice parameters derived of Rietveld analysis using Fullprof program for rhombohedra structures are given in Table 2. A decrease of the crystallite size is observed with increase in the Sr substation up to 0.4 moles. Previous reports showed that formula of sample with x = 0 should be in form of $La^{3+}Mn^{4+}_{0.5}Co^{2+}_{0.5}O^{2-}_3$ to preserve the electro-neutrality of the lattice [6]. The non-uniform changes of values in Table 2 with increasing the substitution suggest the presence of different concentration of various cations Co^{+2}, Co^{+3}, Co^{+4}, Mn^{+4} and Mn^{+3} in samples.

The FT-IR spectra of the $La_{1-x}Sr_xMn_{0.5}Co_{0.5}O_3$ samples calcined at 900°C having ABO_3 structure are shows in Figure 2. In peroveskites ABO_3, the asymmetrical lengthening of the B-O bond of the octahedrons BO_6 appears at 580 cm^{-1} for cubic structure and at 592 cm^{-1} for Rhombohedra structure [4]. The widening of this band and/or the appearance of a shoulder indicates a structure with lower symmetry. The spectra also insinuate the appearance of bands at 1451 and 3429 cm^{-1} that are essentially the asymmetrical and symmetrical lengthening of the O–C–O bond. The presence of impurity phases in the form of carbonates has not been observed in the XRD patterns of the samples, which can be related to the low concentration of these species. These bonds can also be related to the adsorption of carbon dioxide on the surface of samples.

TEM micrographs and particle size distribution of $La_{0.7}Sr_{0.3}Mn_{0.5}Co_{0.5}O_3$ are shown in Figure 3. Fitting of the size distribution histograms by using a log-normal function, the mean diameter calculated is ∼35nm.
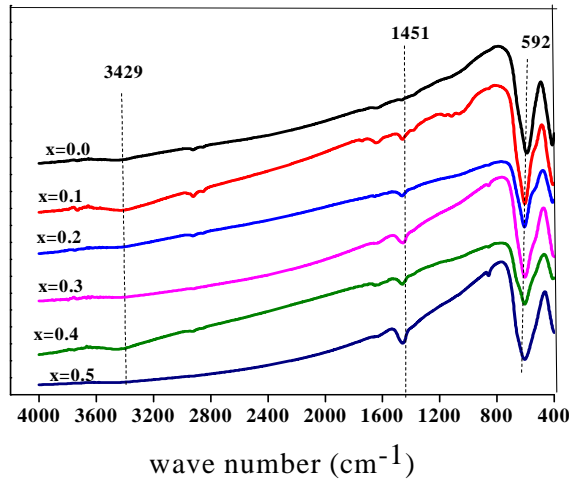
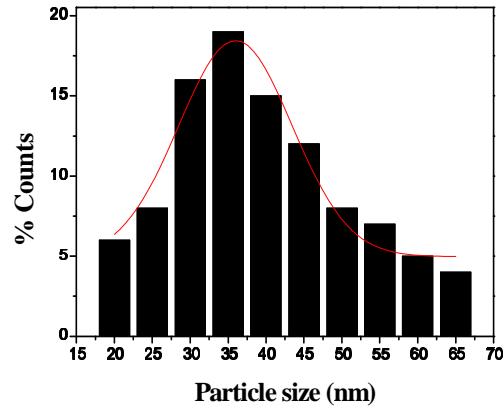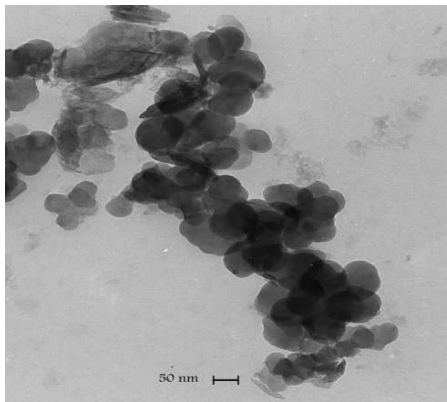**Fig. 2.** FT-IR spectra of $La_{1-x}Sr_xMn_{0.5}Co_{0.5}O_3$

Fig. 3. TEM micrographs and size distribution histograms for $La_{0.7}Sr_{0.3}Mn_{0.5}Co_{0.5}O_3$.

The variations of electrical conductivity (σ) versus temperature (T) obey the Arrhenius equation as follows:

$$(\sigma) = \sigma_\circ \, exp(-\frac{E_c}{RT})$$

Plotting lnσ vs. 1/T, the equation represents a straight line with a slope of $-E_C/R$ and a y-intercept of $ln\sigma_o$. The results of activation energy (E_c) and measured electrical conductivity, reported as σ_{Ox}, σ_{Red} and σ_{Ox}/σ_{Red}, respectively, are summarized in Table 3. Electric conductivity data reported here are the values measured under isothermal steady state conditions at 350 °C. The higher σ_{ox}/σ_{Red} observed for sample x = 0.1 suggest to be the more favorable one for reducibility [7]. Also, the results of energy gap calculation indicate direct band gap for all samples (Table 3). The

non-uniform changes of σ_{ox}/σ_{Red} and energy gap values with increasing the substitution suggest the presence of different concentration of various cations Co^{+2}, Co^{+3}, Co^{+4}, Mn^{+4} and Mn^{+3} in the samples.

Catalytic performance tests of catalysts $La_{1-x}Sr_xMn_{0.5}Co_{0.5}O_3$ for the carbon monoxide oxidation are shown in Figure 4. Also, the results are summarized in Table 4. The results of catalytic performance show that an increase in the Sr substitution provides a better condition for transfer of oxygen to the adsorbed CO on the catalyst surface at the same temperature [7]. Thus, according to the reaction temperature, results show that the sample with x = 0.5 is the best one for the complete CO oxidation. There is an inverse relationship between the crystallite sizes and specific

Table 3. Electric conductivity results of $La_{1-x}Sr_xMn_{0.5}Co_{0.5}O_3$

Sample	$\sigma_{ox}\times 10^6$ (Ω^{-1})	$\sigma_{Red}\times 10^6$ (Ω^{-1})	σ_{Ox}/σ_{Red}	E_c (kCal/mol)	E_{gap} (eV)
x = 0.0	3.31	2.83	1.17	15.95	2.02
x = 0.1	248.32	156.25	1.59	12.91	1.98
x = 0.2	1178.34	1180.84	0.998	11.03	1.96
x = 0.3	2070.07	1801.31	1.149	17.54	1.9
x = 0.4	1698.08	1449.27	1.172	16.99	1.9
x = 0.5	2956.72	2751.43	1.075	16.42	2.69

Table 4. Catalytic performance (%), CO oxidation temperatures (^{o}C), for $La_{1-x}Sr_xMn_{0.5}Co_{0.5}O_3$

Sample	10%	50%	95%
x = 0.0	178	285	322
x = 0.1	239	277	330
x = 0.2	160	178	248
x = 0.3	129	200	223
x = 0.4	71	158	198
x = 0.5	120	165	175
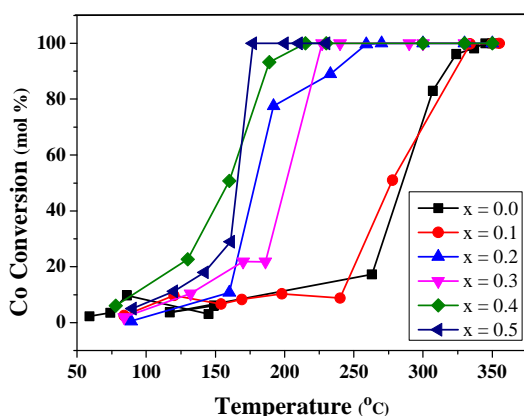
Fig. 4. The curves of CO conversion versus temperature for $La_{1-x}Sr_xMn_{0.5}Co_{0.5}O_3$ nanocatalysts.

surface area of the samples [8]. In addition, it is known that higher activity should be related to the higher specific surface area and lower crystallite sizes [2]. Consequently, the structural, redox, and catalytic results suggest that the lower temperature conversion of CO for x = 0.5 can be mainly attributed to higher specific surface due to lower crystallite sizes.

4. Conclusions

The rietveld refinement of the XRD patterns performed using Fullprof software show a cubic structure (Pm3m space group) for *x* = 0.0 and a rhombohedra structure (R-3c space group) for the Sr substituted $La_{(1-x)}Sr_xMn_{0.5}Co_{0.5}O_3$ samples. The results of

$\sigma_{Ox.}/\sigma_{Red}$, activation energy ($E_c$) and band gap energies indicate non-uniform variations with increase in the Sr substitution, whereas the crystallite size and unit cell parameters decrease progressively. An increase of the Sr substitution up to 0.5 enhances the performance of the samples in the low-temperature conversion of CO to CO_2. Consequently, the structural, redox, and catalytic results suggest that the lower temperature conversion of CO for x = 0.5 can be mainly attributed to higher specific surface due to lower crystallite sizes.

References

1. U. G. Singh, J. Li, J. W. Bennett, A. M. Rappe, R.Seshadri, S. L. Scott, "A pd-doped perovskite Catalyst, $BaCe_{1-x}Pd_xO_{3-\delta}$, for CO oxidation", J. Catal., Vol. 249, 2007, pp. 349-358.
2. E. Frozandeh-Mehr, A. Malekzadeh, M. Ghiasi, A. Gholizadeh, Y. Mortazavi, A. Khodadadi, "Effect of partial substitution of lanthanum by strontium or bismuth on structuralfeatures of the lanthanum manganite nanoparticles as a catalyst for carbon monoxide oxidation", Catal. Commun., Vol. 28, 2012, pp.32–37.
3. V.A. Ryzhov, A.V. Lazuta, P.L. Molkanov, V.P. Khavronin, A.I. Kurbakov, V.V. Runov, Ya.M. Mukovskii, A.E. Pestun, R.V. Privezentsev, "Comparative study of heterogeneous magnetic state above T_C in $La_{0.82}Sr_{0.18}CoO_3$ cobaltite and $La_{0.83}Sr_{0.17}MnO_3$ manganite", J. Magn. Magn. Mater., Vol. 324,

2012, pp.3432–3436.
4. G. Pecchi, et al., "Thermal stability against reduction of LaMn$_{1-y}$Co$_y$O$_3$ perovskites", Mater. Res. Bull., Vol. 44, 2009, pp. 846–853.
5. A. Gholizadeh, N.Tajabor , "Influence of N$_2$- and Ar-ambient annealing on the physical properties of SnO$_2$:Co transparent conducting films", Mater. Sci. Semicond. Process., Vol. 13, 2010, pp. 162–166.
6. I. P. Nisha, S. S. Pillai, K.G. Suresh and M.R.Varma, "Influence of Dy addition on themagnetocaloric effect of La$_{0.67}$Ca$_{0.33}$Mn$_{0.9}$V$_{0.1}$O$_3$ ceramics", J. Magn.

Magn. Mater., Vol. 324, 2012, pp. 37–43.
7. M. Ghiasi, A. Malekzadeh, "Synthesis of CaCO$_3$ nanoparticles via citrate method and sequential preparation of CaO and Ca(OH)$_2$ nanoparticles", Cryst. Res. Technol. Vol. 47, 2012, pp. 471-47.
8. Z. Gholipour, A. Malekzadeh, R. Hatami, Y. Mortazavi, A.Khodadadi, "Oxidative coupling of methane over (Na$_2$WO$_4$+Mn or Ce)/SiO$_2$ catalysts: In situ measurement of electrical conductivity", J. Nat. Gas Chem. Vol. 19, 2010, pp. 35-42.